

Design of Receiver Used for Passive Millimeter Wave Imaging System

Bao-Hua Yang^{*a}, Zhi-Ping Li^b, Tong-Fei Yu^c, Jin Zhang^d, Xian-Xun Yao^e, An-Yong Hu^f,
Cheng zheng^g, Jun-Gang Miao^h

School of Electronic and Information Engineering, Beihang University, 100191, Beijing, China

*Corresponding author, e-mail: yangbaohua728@163.com^a, zhiping_li@buaa.edu.cn^b,
15210809120@163.com^c, zhangjin850224@139.com^d, yaoxianxun@126.com^e, hay800906@126.com^f,
zhengcheng@sina.com^g, jmiaobremen@126.com^h

Abstract

As millimeter wave (MMW) electronic technologies have matured, the MMW imaging using for human security inspection is emerging as an effective approach to imaging through obscuring materials, such as clothing for concealed weapons detection or plastic mines. This paper introduces temperature sensitivity firstly and then the fringe-washing functions are derived which decide the structure the antenna array and the receivers of the system BHU-2D. Finally, the fringe-washing functions and their phases are calculated from the frequency responses of 24-receiver, they all show good consistency of the receivers which also can be proved from the test results of receivers. From the final imaging of our system, the 1-2K temperature sensitivity is realized successfully.

Keywords: receiver, aperture synthesis, radiometer, fringe-washing function

Copyright © 2014 Institute of Advanced Engineering and Science. All rights reserved.

1. Introduction

Since the aperture synthesis was introduced into microwave radiometry of the earth, steady progresses have been made for more than 50 years [1]. Many aperture synthesis radiometers in earth remote sensing application have developed such as ESTAR (Electronically Scanned Thinned Array Radiometer) and MIRAS (Microwave Imaging Radiometer with Aperture Synthesis) [2-3]. All of their applications were aimed at remote sensing.

The applications of microwave systems for near-field zone noncontact inspection was very appealing recently, which ranged from civil and industrial engineering to biomedical analysis [3-5]. Since 1990s, many companies have developed several types passive millimeter wave (PMMW) imaging systems whose applications were aimed at human inspection at harbor and airport for example Millivision.co, Sago and QinetiQ [7-8]. Owing to their passive MMW receiver, these systems maybe have fewer harm for human healthy than the tradition X ray system. The Electromagnetics Laboratory of Beihang University also engaged in the research on the aperture synthesis MMW radiometer. A series of 8mm band instrument with disk antennas has been developed for application of human security apparatus that is BHU-2D [9-12]. The imaging principle of synthetic aperture interferometric radiometer (SAIR) and background cancellation method have been stated by our lab [13].

SAIR confronts decorrelation or so-called fringe-washing effects due to wide field of view requirement. These effects have been considered detailedly in this paper.

2. Instrument Description

The dangerous materials can be checked with the security inspection device based on the brightness temperature difference between them and human bodies by PMMW technology. When the dangerous materials are made of metal, plastic or ceramic, their brightness temperature differences with human bodies, named temperature sensitivity, are about 6-8 k and 1-2k respectively according to their emissivities.

$$\Delta T = \left| e_1 - e_2 \right| \left| T_p - T_i \right| = \frac{T_{SYS}}{\sqrt{B\tau}} = \frac{T_A + T_R}{\sqrt{B\tau}} \tag{1}$$

$$\approx \Omega_p \Delta_s \frac{T_A + T_R}{\sqrt{B\tau_e}} \frac{\alpha_W}{\alpha_F} \alpha_{LO} \sqrt{N_V} = \frac{1}{\eta} \frac{T_A + T_R}{\sqrt{B\tau_e}} \frac{\alpha_W}{\alpha_F} \alpha_{LO} \sqrt{N_V}$$

Where the parameters T_A , T_R , B and τ is the antenna temperature, the noise temperature, the system bandwidth and the integration time respectively, η is the aperture efficiency of unit antenna, α_w is the factor of window function, α_{LO} is the LO factor α_F is the filter factor, N_V is the sampling number of rectangular visibility function, τ_e is the equivalent integration time of 1bit/2level digital correlation, the temperature sensitivity of the system is about 1.5 K from the above formula [12]. As can be seen, the item $B\tau$ is the only variant. From the formula (2) it is the same for the fringe-washing function which means the decorrelation effect of the interferometric aperture synthesis radiometer due to wide field of view requirement.

$$\tilde{r}_{ij}(\tau) = \text{sinc}(B\tau) \tag{2}$$

So, the fringe-washing function is described by asinc-function in the case, which is only dependent on bandwidth of thereceivers. Forcomparison, Figures 1 shows this theoretical fringe-washingfunction for MIRAS receivers (bandwidth 19 MHz), for HUT-2D receivers (bandwidth 7 MHz) [13] and for our receivers of BHU-2D (bandwidth 400MHz).

The maximum delay form the edge of the field of view of BHU-2D is $\pm 0.4\text{ns}$, as explained in Section 3. For comparison, the maximum delay in the case of MIRAS and HUT-2D is $\pm 12.5\text{ ns}$ and $\pm 6.1\text{ ns}$ respectively. From Figure 2 it can be seen that maximum attenuation caused by the theoretical fringe-washing function at these delays are 0.090 for MIRAS, 0.005 for HUT-2D and 0.21 for BHU-2D.

In practice, the frequency responses of receivers are not rectangular, they have ripple on the passband and finite attenuation on the stopband. They are also non-symmetric causing formula (2) to the complex. So they are not similar from one to another. The fringe-washing function $r_{ij}(\tau)$ is defined as formula (3) [13-16].

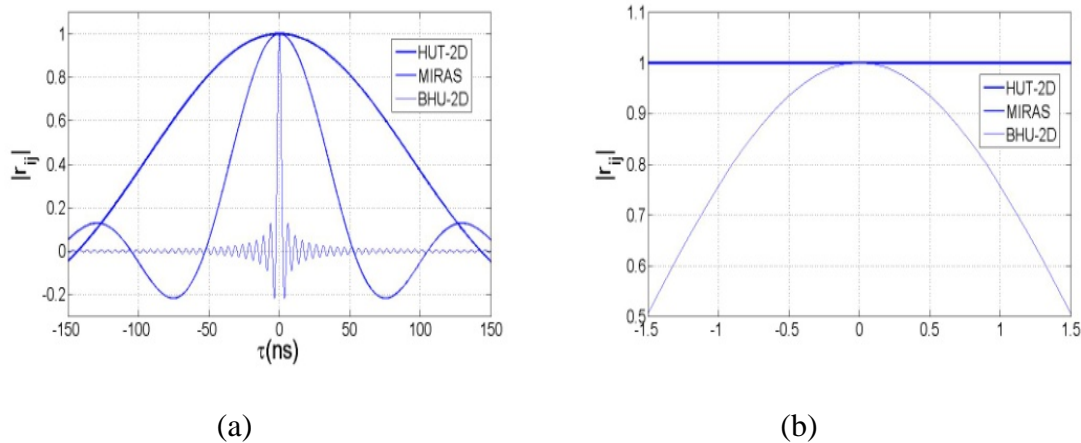


Figure 1. Fringe-washing functions of MIRAS, HUT-2D and BHU-2D receivers, assumed having rectangular frequency responses, (b) is zoomed from (a)

$$\tilde{r}_{ij}(\tau) = \frac{1}{\sqrt{B_i B_j}} \int_{f_0}^{\infty} H_{n,i}(f + f_0) H_{n,j}^*(f + f_0) e^{j2\pi f \tau} df \tag{3}$$

Where H_n is the normalized frequency responses of receivers i and j .

The aperture synthesis millimeter waveradiometer is a two-dimensional imaging radiometer having 24 antenna/receiver elements. It consists of a disk antennaarray, receivers, a data acquisitionsubsystem, and a PC. Figure 2 illustrates the antennaarray and the receivers of the instrument.

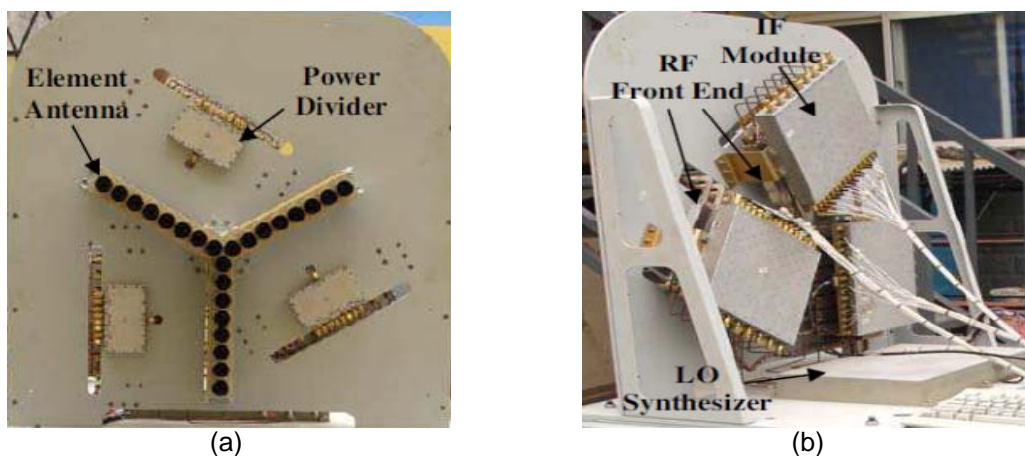


Figure 2. Illustrates the antennaarray and the receivers of the instrument

The complete instrument consists of 24 K_a -band receivers which are arranged in Y-shaped configuration. The receiver distance is 3.07λ , double-side bandwidth is 400MHz, the center frequency is 34.1GHz and the longest baseline length of the complete is 0.37m. At the edge of field of view (20°), these characteristics led to maximums delay of ± 0.4 ns. After the I/Q demodulated, the signal is digitized in 1-bit. All parameters are tabulated in Table 1.

The signals collected by the antennas are fed into a group of dual-conversion receivers with I/Q demodulators. From Figure 2, each receiver consists of a RF front end and an IF module. The down-converters in the RF front end and the IF module is operated in single sideband mode and double sideband mode respectively. Thenominal gain and noisetemperature ofthe receivers are 87 dB and 370K respectively.

Table 1. The Main Parameters of BHU-2D

Parameter	Power (kW)
Center Frequency	34.1GHz
Bandwidth	400MHz
LO Frequency	32GHz (for RF front end) 2GHz (for I/Q demodulator)
Field of View	20°
Temperature Sensitivity	$\sim 1K(0.5s$ Integration time) $\sim 3K(0.05s$ Integration time)
Geometry of Antenna Array	Y-shaped
Number of Receiver Elements	24
Antenna Element Spacing	27mm(3.07 wavelengths)
Number of Baselines	427
Number of Correlators	924
Number of Cross Correlators	852
Calibrations	Noise Injection(External point source) Background Cancellation

In order to equalizethe gain between channels, the gain of IF module can be adjustedby a variable attenuator. For the purpose of reducing the dimension of the instrument,the receivers are installed parallel to the array. The RF front end andthe IF module

are installed in Figure 2 (a) and (b). As is shown in Figure 3, the structure of the system can be seen.

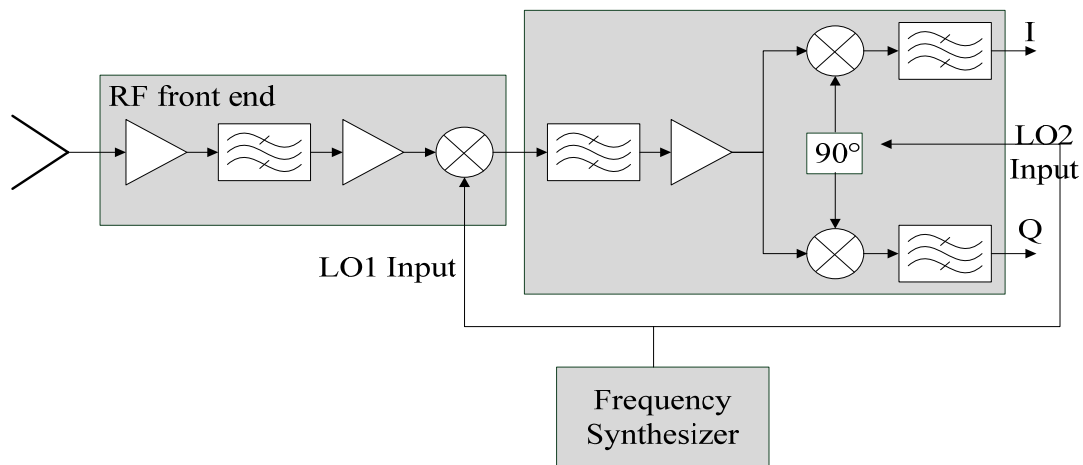


Figure 3. Block diagram of the receiving element.

3. Results of Calculation and Measurement

3.1. Calculation of the Fringe-Washing Function

The fringe-washing function of 24 receivers of BHU-2D are calculated as follows. Frequency responses of 24 BHU-2D receivers were measured using a Vector Network Analyser firstly. Forty eight measured frequency responses (only Q channels are shown for convenience) are shown in Figure 4.

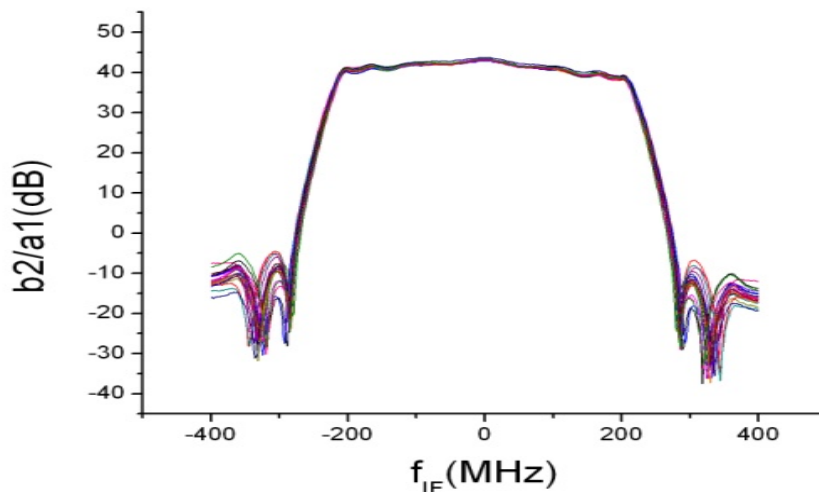


Figure 4. Frequency responses of 24 BHU-2D receivers (Q channels)

From the measured results it is straightforward to calculate the fringe-washing function according to (3). Forty eight receivers form altogether 564 baselines, whose fringe-washing functions are shown in Figure 5(a) (moduli) and (b) (phase). In order to make their absolute value equals to 1 and their phase equals to 0 at $\tau = 0$, these fringe-washing functions are the ones normalized

From figure 5(a) we can see that the attenuation is approximately 0.1 around 0.4 ns. Its not far away from the estimation of (2), the difference between the minimum and maximum attenuation is almost 0.06. From figure 5(b) we can see that the fringe-washing function phase gets values approximately $\pm 0.5^\circ$ between ± 0.4 ns.

3.2. Measurement Results of Receivers

In order to get good performance of the system, the consistency of 24 I or Q and between I and Q channels is very important. From figure 4, the good consistency of 24 Q channels was get. The consistency between I and Q channels can be get from the figure 6. From figure 5 (a) and (b) show the amplitude error of 24-receiver I/Q channels and its average value, the results vary from -0.54 to +0.69 dB, its most average value is 0.5 dB.

The intermediate receiver structure is double-sideband, so the orthogonal phase difference of I/Q channel output signals in bandwidth has two parts, its bandwidth is 400MHz from -200 to 200 MHz. From figure 7 shows that the orthogonal phase difference of I/Q channel output signals is between -4.5° to 9° and their average value vary from 0.34° to 3.75° , it shows the good orthogonal phase of the I/Q channels.

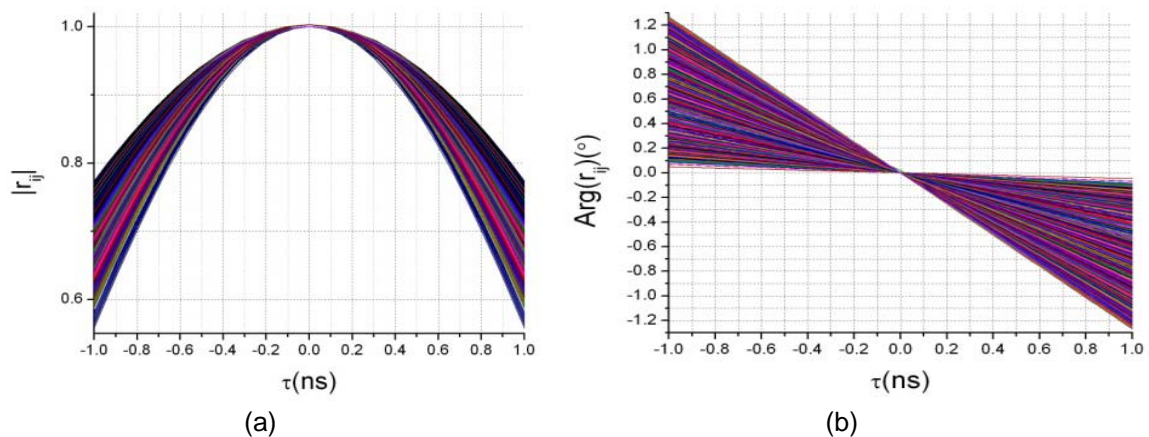


Figure 5. Fringe-washing functions of BHU-2D 24-receiver. (a) Moduli of 1128 fringe-washing functions; (b) Phases of 24 fringe-washing functions

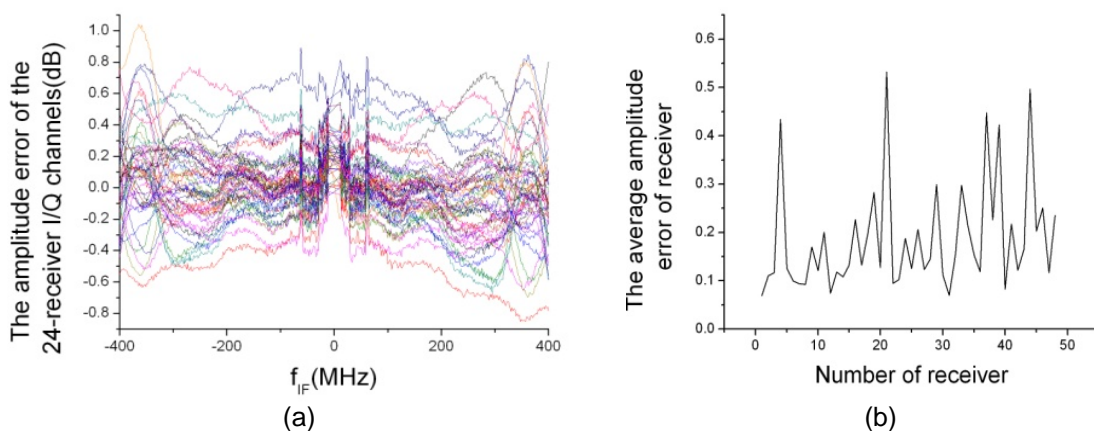


Figure 6. The amplitude consistency of 24-receiver, (a) the amplitude error of the 24-receiver I/Q channels; (b) the average value of I/Q channels.

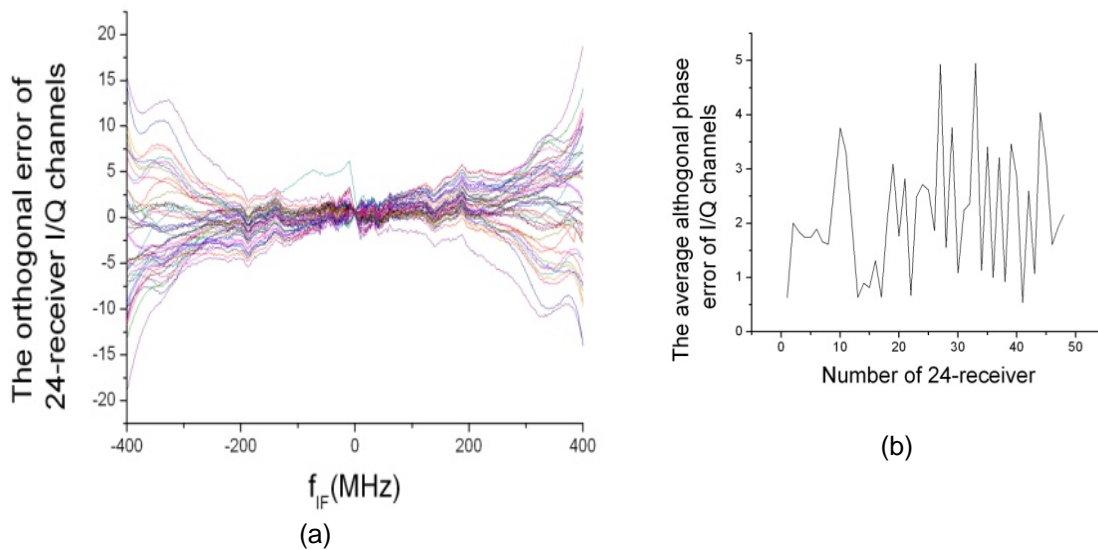


Figure 7. The orthogonal error of 24-receiver I/Q channels, (a) the orthogonal error of I/Q channels; (b) its average value of orthogonal error.

3.2. Measurement Results of System

To check the instrument performance, we take several scenes that people take different materials such as a bag of oatmeal with a size of 20*17.5cm

From Figure 8 it shows that the conceal weapon and some dangerous materials can be detected by the system such as glue and powder. Their right figures of figure 8 (a) , (b) and (c) can be obtained from the subtract of the left two. We see that the brightness temperature difference of 1-2k can be detected successfully and the requirement of temperature sensitivity is realized.

4. Conclusion

The aperture synthesis millimeter waveradiometer used for human security inspection was designed by the Electromagnetics Laboratory of Beihang University. From the results of frequency responses, the fringe-washing function, and final performance, our requirements for the system have been realized which has good performance of the amplitude and orthogonal phase consistency and 1-2 K temperature sensitivity. The next generation of our system is U-shaped SAIR with 48 receivers.

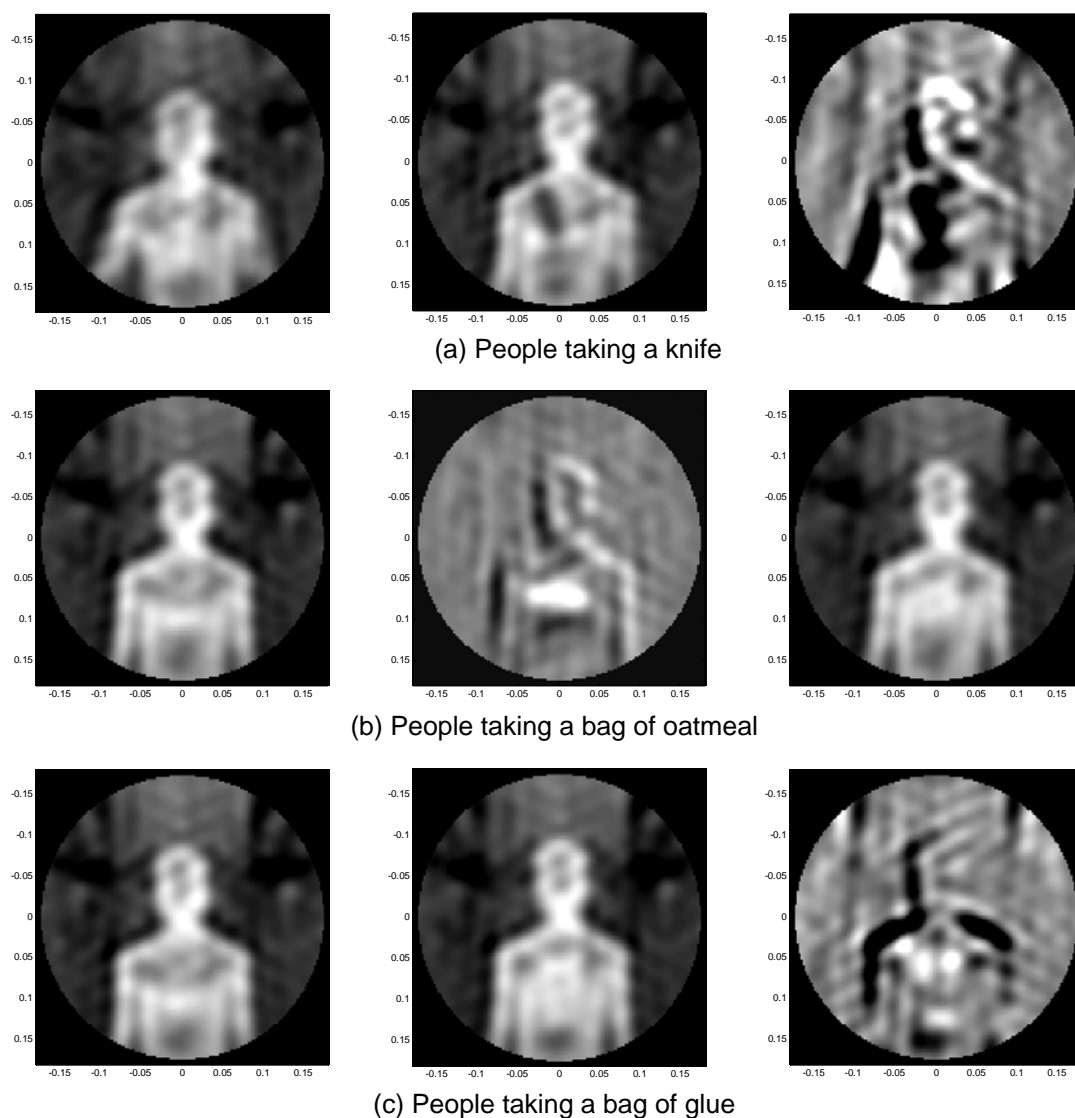


Figure 8. The image of people with different materials, (a) people taking a knife; (b) people taking a bag of oatmeal; (c) people taking a bag of glue.

References

- [1] R Thompson, JM Moran, and GW Swenson Jr. *Interferometry and Synthesis in Radio Astronomy*. 2nd ed. John Wiley & Sons. New York. 2001: 12-40.
- [2] B Tanner, WJ Wilson, and BH Lambrigsten et al..Initial results of the geostationary synthetic thinned array radiometer (GeoSTAR) demonstrator instrument. *IEEE Trans. Geosci. Remote Sens.* 2007; 45(7): 1947-1957.
- [3] Simorangkir Roy BVB, Munir Achmad. Numerical design of ultra-wideband printed antenna for surface penetrating radar application. *Telkomnika Indonesian Journal of Electrical Engineering*. 2011; 9(2): 341-350.
- [4] B Tanner, BH Lambrigsten, TM Gaier, F Torres. *Near field characterization of the GeoSTAR demonstrator*. Proc IEEE IGARSS, Denver, Co, USA. 2006; 2529-2532,.
- [5] Ding H. Application of Wireless Sensor Network in Target Detection and Localization. *TEKOMNIKA Indonesian Journal of Electrical Engineering*. To be published in 2013; 11(10).
- [6] WANG Nan-nan, QIU Jing-hui, DENG Wei-bo. Development Status of Millimeter Wave Imaging Systems for Concealed Detection. *Infrared Technology*. 2009; 31(3): 129-135.
- [7] Gordon N Sinclair, Rupert N Anderton, and Roger Appleby. *Outdoor Passive Millimeter Wave Security Screening*. Security Technology 2001 IEEE 35th International Carnahan. 2001: 172-179.

- [8] John A Lovberg, Chris Martin, and Vladimir Kolinko. *Video-Rate Passive Millimeter-wave Imaging Using Phased Arrays*. Microwave Symposium 2007, IEEE/MTT-S International. 2007: 1689-1692.
- [9] Yong Xue, Jungang Miao, Guolong Wan, Anyong Hu, Feng Zhao. *Prototype development of an 8mm band 2-Dimensional aperture synthesis radiometer*. 2008 International GeoScience and Remote Sensing symposium. Boston. 2008: 413-416.
- [10] Anyong and Miao Jungang. Prototype development of an 8mm-band two dimensional interferometer synthetic aperture radiometer. Mechanic Automation and Control Engineering (MACE), 2011 Second International Conference. Baotou. 2011: 1487-1490.
- [11] Yong Xue, Jungang Miao, Guolong Wan. *Development of the disk antenna array aperture synthesis millimeter wave radiometer*. International Conference on Microwave and Millimeter Wave Technology. ICMMT 2008. 2008; 2: 806 – 809.
- [12] Bao-Hua Yang, Ghulam Mehdi, Anyong Hu. The Round-Ended Design and Measurement of All Symmetric Edge-Coupled Bandpassfilter. *Progress In Electromagnetics Research C*. 2013; 38: 191-203.
- [13] Cheng Zheng, Xianxun Yao, Anyong Hu, and Jungang Miao. A Passive Millimeter-Wave Imager Used For concealed Weapon Detection. *Progress In Electromagnetics Research B*. 2013; 46: 379-397.
- [14] Torres F, Tanner AB, Brown ST, et al. Analysis of Array Distortion in a Microwave Interferometric Radiometer. *Application to the GeoSTAR Project*. *IEEE Trans. Geosci. Remote Sens.* 2007; 45(7): 1958-1966.
- [15] Juha Kainulainen, Kimmo Rautiainen, Martti Hallikainen, *Experimental Verification of Fringe-washing Calibration Techniques in Large Aperture Synthesis Radiometers*. IEEE MicroRad. San Juan. 2006: 13-17.
- [16] Xianxun Yao, Zhiping Li, Cheng Zheng, Baohua Yang. Analysis and Correction of the Inter-channel Mismatch in Synthetic Aperture Radiometer. *TELKOMNIKA Indonesian Journal of Electrical Engineering*. To be pulished in Dec. 2013.